Supplementary Information: Simulating chronic wasting disease spread in California after the initial detection

Cesar Herraiz[1,2], Carlos González-Crespo[2*], Brandon Munk[3], Alexander Heeren[3], Pelayo Acevedo[1], Beatriz Martínez-López[2]

[1] Health and Biotechnology Research Group (SaBio), Institute for Game and Wildlife Research (IREC), CSIC-JCCM-UCLM, 13071 Ciudad Real, Spain

[2] Center for Animal Disease Modeling and Surveillance (CADMS), Department of Medicine & Epidemiology, School of Veterinary Medicine, University of California, Davis 95618 CA, USA

[3] California Department of Fish and Wildlife (CDFW), Wildlife Health Laboratory (WHL), Rancho Cordova, CA 95670, USA

*Corresponding author:
Carlos González-Crespo
cgonzalezcrespo@ucdavis.edu

Index

Appendix 1: ODD Protocol

1.1 Purpose

The purpose of the model is to simulate the spatiotemporal dynamics of CWD in mule deer in the state of California. To achieve this, the model comprises two main modules:

1. The ecological module, which pertains to the host, and whose purpose is to simulate the mule deer population in California over time and space, considering its response to both natural phenomena, such as fires or droughts, and anthropogenic factors, such as hunting. This module is comprised of two submodules. The first submodule pertains to the environment and encompasses data and processes such as habitat suitability, scavenging pressure, fires and droughts. The second submodule pertains to the host and includes demographic, social, and behavioral information about mule deer, such as natality and mortality, migrations and grouping patterns.
2. The epidemiological module, which is related to the pathogen, and whose purpose is to examine the spread of CWD over time in the mule deer population. This module interacts with the ecological one. The evolution of the deer population affects the pathogen spread, which in turn affects the population by causing mortality.

1.2 Entities, state variables, and scales

The model comprises three agents as entities: deer, carcass, and grid cells. The discretization of the space into grid cell agents allows some processes to be programmed at the cell level, thereby reducing the computational cost and increasing the ability to apply a complex model to large scales.

Each deer is defined by 14 state variables related to location, age, sex, fawning, grouping, migratory behavior, and CWD infection status. When an infected deer dies, it becomes a carcass agent, with the location and the days of persistence in the environment as state variables. Grid cells have 9 state variables related to habitat suitability, carrying capacity (K), deer range (year-round, winter, summer, or out of the range), deer abundance (N), infectious deer carcass abundance, CWD prevalence, scavenging pressure, hunting pressure and

whether the cell has been damaged by fire. The entities included in the model and their state variables are shown in Table S1.

The spatial extent of the grid encompasses the California state, being each grid cell a 10 km x 10 km size square (100 km^2). The model has a daily time step, starting in the middle of the summer (day = 213; August 1st).

Table S1. Entities and their states variables included in the simulation.

Entity	State variable	Description
Deer	*cell*	id of the grid cell in which deer is located
	residence	id of the grid cell where deer resides
	sex	1 for male and 0 for female
	age	Age in days
	class	1 if fawn, 2 if yearling, 3 if adult, 4 if old
	fawning	1 if pregnant female, 0 otherwise
	mother	id of the mother
	group	id of the group to which it belongs
	solitary	1 if solitary, 0 otherwise
	migratory	1 if it belongs to a migratory population, 0 otherwise
	susceptible	1 if uninfected, 0 otherwise
	exposed	1 if infected but not infectious, 0 otherwise
	infected	1 if infected and infectious, 0 otherwise
	clinical	1 if infected with clinical signs, 0 otherwise
Carcass	*loc*	id of the grid cell in which the deer infectious carcass is located
	removal	Number of days the carcass remains in the environment
Grid cell	*N*	Mule deer abundance
	migra	Mule deer range: 1 if summer range, 2 winter range, 3 if year-round, -1 otherwise
	K	Number of mule deer that the grid cell can shelter
	weight	Cell resistance
	huntpressure	Proportion of the population annually harvested
	prevalence	CWD prevalence in the cell
	ncarcass	Number of deer infectious carcasses in the cell
	scavengers	1 to 5 depending on the number of present scavengers' species
	daysburnt	Days elapsed since the cell was burnt

1.3 Process overview and scheduling

Processes referred to the deer agent in the model are related to: 1) mule deer population dynamics; and 2) CWD disease dynamics in the mule deer population. Population dynamics processes include aging, natural mortality, hunting mortality, fawning, seasonal group dynamics, yearling dispersal, and seasonal migrations.

The CWD disease dynamics processes include pathogen transmission or exposition and CWD-induced mortality.

Processes related with the mule deer population dynamics are scheduled as follows (Ahlborn & White 2006; Mejia-Salazar *et al.* 2017; Monteith *et al.* 2011): On December 16th (day = 350) early gestation (EG) starts, and large mixed groups are formed. On April 1st (day = 91) late gestation (LG) period starts, during which males separate from females and young individuals. Departure from winter range areas to summer range (spring migration) begin in middle April (day = 105). Fawning (F) starts on May 16th (day = 136), resulting in the formation of the smallest groups of the year. Females go apart for giving birth, while fawns from the previous year separate from their mothers' group and disperse. On August 1st (day = 213) pre-rut (PR) period begins, and males start joining females with fawns. Females without fawns remain in small groups. Hunting mortality occurs between August 14th (day = 226) and November 7th (day = 311). Fall migration commences in mid-October (day = 288). Rut (R) period begins on November 1st (day = 305). Aging and natural mortality occur every step. The day starts from 0 (1st January) after it reaches 365 (31st December).

With regard to the CWD processes scheduling, prion shedding commences 6 to 9 months (180 to 270 days) after infection (Plummer *et al.* 2017; Tamguney *et al.* 2009), thereby enabling direct transmission and environmental deposition. Clinical signs manifest approximately 490 days after infection (Johnson *et al.* 2011; Williams 2005). Death by disease takes place 14 to 120 days after the onset of clinical signs (Williams 2005). Following death, infected deer become a carcass agent, which remains infectious (Miller *et al.* 2004). The only process considered for the carcasses is their disappearance. The time carcasses remain in the environment depends on the season and scavenging pressure (Jennelle *et al.* 2009).

The processes referred to the grid cells are droughts, wildfires, and the diffusion of CWD across neighboring cells. Drought has a given probability of occurring at the start of the simulation and can last for a number of days derived from a uniform distribution between 365 and 1460 days (1 to 4 years; Miller *et al.* 2022). During the summer months, wildfires may occur in cells with a certain probability, affecting carrying capacity (Bristow *et al.* 2020; Sparks *et al.* 2018).

1.4 Design concepts

1.4.1 Basic principles

Density dependence in mule deer was assumed to be related with the carrying capacity in the winter range, which entails an effect on fawn survival in winter but not on adult survival (Bergman *et al.* 2015). The buck:doe ratio was considered not to affect the birth rates since no severe decline in productivity was found as a response to the sex ratio (White *et al.* 2001). Predation, primarily by coyote (*Canis latrans*) and mountain lion (*Puma concolor*), could influence mortality rates in the overall population, particularly in fawns. However, several studies have shown changes in predator communities entailing compensatory effects, leading to the absence of changes in population trends (for further information, see Forrester & Wittmer 2013). Therefore, no changes in mule deer demography based on predator community composition were assumed in the model.

This model assumes that CWD can be transmitted through direct animal contact or through the environmental presence of the prion, either in the soil or in an infectious carcass (Miller, Hobbs & Tavener 2006). Furthermore, it assumes a CWD diffusion process from where the outbreak originates (Jennelle *et al.* 2014). Vertical transmission was omitted in the model since it is unusual (Miller & Williams 2003) and seems no to have an effect on the disease dynamics (Potapov *et al.* 2013). In addition to mortality due to CWD, the model assumes an increase in mortality of infected deer due to greater susceptibility to predation, vehicle kill, dehydration, or hypothermia during winter months (Miller *et al.* 2008; Otero *et al.* 2021).

Long-range movements may also play an important role in the spread of the pathogen to farer areas (Diefenbach *et al.* 2008; Garlick *et al.* 2014). Therefore, dispersal and migration were incorporated into the model. Mule deer populations in California can be resident or migratory (Ahlborn & White 2006). Resident populations were assumed to remain in the same cell throughout the year, while migratory populations were assumed to move entirely from summer to winter range cells in fall migration, returning to the cell where they were born in spring migration (van de Kerk *et al.* 2021). Dispersion is carried out by yearlings, mainly males but also females (Robinette 1966), Displacements can occur in any direction within the range (Hamlin & Mackie 1989). Cells selected for migratory displacements were assumed to depend on habitat suitability, slope, and its traditional use as migratory corridors. Upon reaching the target cell, the probability of the deer remaining in that

cell or moving on to another suitable cell is assumed to depend on the *N* and *K* values of the cell, leading to dispersion towards another cell when *N* approaches *K*.

The model assumes that drought leads to an increase in mortality and in the probability of wildfires (Jackson *et al.* 2021; Littell *et al.* 2016; Schuyler, Dugger & Jackson 2018). With regard to wildfires, it is assumed that when they occur, the environmental prion load of the cell is eliminated (Lee 2023). Moreover, it is postulated that wildfires have an effect on the cell's *K*, reducing it to a minimum during the first year after the fire and almost doubling during the second year, then stabilizing over the next three years (Bristow *et al.* 2020; Sparks *et al.* 2018).

1.4.2 Emergence

The CWD spread emerges from the model based on the mule deer population, grouping and movement patterns, and on transmission dynamics. Mule deer mortality is also influenced by population abundance and CWD prevalence rates, so mule deer population dynamics itself also emerges from the model.

1.4.3 Adaptation

The mule deer adapt their behavior based on *N* and *K*. When *N* approaches *K*, either due to an increase in population or a sharp reduction in *K* as a result of a wildfire, the mule deer disperse to other cells that have the capacity to accommodate them.

1.4.4 Sensing

The mule deer agents sense the state variables of the grid cell agents, which influence the probability of being hunted, the destination and movement cells for migratory and dispersal movements, and the probability of infection through environmental prion load or the presence of infectious carcasses. Conversely, grid cells also sense mule deer agents, as they sense the number of deer they contain and how many of them are infected, thus determining N, the prevalence of CWD, and the prion load. Moreover, they also sense the presence of infectious carcass agents. Finally, there is also sensing among the mule deer agents themselves, which determines group dynamics and transmission within them, and among the grid cell agents themselves, determining the spread of fires or the diffusion of the pathogen between cells.

1.4.5 Interaction

Deer agents can interact being able to entail pathogen transmission if one of them is infected and the other one is not. Deer agents can interact with infected deer carcasses agents being able to acquire the pathogen if they are not infected. Deer agents also interact with the grid cell agents, as the prion load of each cell is determined by infected deer that are or have been in it. This prion load can, in turn, lead to the infection. Additionally, grid cell agents interact with each other, as the CWD diffusion process considers new infection in a cell based on the prevalence of neighboring cells.

1.4.6 Stochasticity

Natality (i.e., the number of offspring per female and the occurrence of twins, as well as the sex of the offspring), mortality (both natural and hunting-related mortality), and dispersal, are based on probabilities that affect each individual, and therefore are stochastic processes. Hunting is also a stochastic process since hunting pressure is defined by a Gamma distribution. These demographic processes condition mule deer abundance, having an effect on cell selection during migration and thus making this process also stochastic. Moreover, the day on which each individual migrates is also stochastic, conditioning the abundance on the target cell at the time of its arrival, and therefore influencing cell selection. Group dynamics is also a stochastic process in which size is provided as a range and the members are randomly selected based on the size and sex and age ratios for each season. All transmission processes and durations of each infection status are stochastic as they are based on probabilities and variable time intervals. Drought has a probability of occurring at the beginning of the simulation, and its duration is variable. Each cell has a certain probability of being burnt by a wildfire each summer.

1.4.7 Collectives

Deer agents are organized in social groups that fluctuate in size and sex and age ratios seasonally. The transmission processes of CWD differ within and outside of these groups.

1.5 Initialization

The initial sex and age ratios of the mule deer population are shown in Table S2. All deer are initially susceptible to infection. The outbreak initiates with the infection of an adult male, based on observed infection rates (Miller & Conner 2005; Osnas *et al.* 2009). The location and start date of the outbreak can be selected for

each simulation. Mule deer demographic and epidemiological parameters employed for the simulation are described in Tables 3 and 4, respectively.

Table S2. Initial proportion of the population by sex and age based on Furnas *et al.* (2018); Rittenhouse, Mong and Hart (2015); Wood *et al.* (1989).

Initial proportion of the population	
Fawn male (0 - 1 year)	0.17
Fawn female (0 - 1 year)	0.17
Yearling male (1 - 2 years)	0.11
Yearling female (1 - 2 years)	0.14
Adult male (2 - 9 years)	0.09
Adult female (2 - 11 years)	0.25
Old male (9 - 12 years)	0.02
Old female (11 - 16 years)	0.05

Table S3. Mule deer demographic parameters. PR is the pre-rut period, R is the rut period, EG is the early gestation period, LG is the late gestation period, and F is the fawning period.

Parameter	Description	Value	Source
preg	Proportion of females that get pregnant (yearling; adult; old)	0.6; 0.87; 0.8	Bender and Hoenes (2018); Monteith *et al.* (2014); Taylor (1996)
fawnsex	male:female sex ratio at parturition	1:1	Taylor (1996)
twinp	Twin probability given pregnancy (yearling; adult; old)	0.07; 0.87; 0.29	Bender and Hoenes (2018); Bishop *et al.* (2010); Monteith *et al.* (2014); Taylor (1996)
fawnsurv	Fawn survival rate (F and PR; other seasons)	0.44; 0.61	Forrester and Wittmer (2013)
starv	Fawn survival to starvation rate	Eq. 3	Adapted from Potapov *et al.* (2013)
survf	Yearling and adult female deer survival rate	0.85	Forrester and Wittmer (2013)
survm	Yearling and adult male deer survival rate	0.78	Bishop *et al.* (2005); Forrester and Wittmer (2013)
oldsurv	Old deer survival rate (male; female)	Eq. 4; Eq. 5	Gross and Miller (2001)
k_{hunt}	Shape parameter of gamma function for hunting pressure (adult/old male; adult/old female; yearling male; other)	12.325; 12.327; 12.331; 0	Numerically optimized from CDFW harvest statistics
θ_{hunt}	Scale parameter of gamma function for hunting pressure (adult/old male; adult/old female; yearling male; other)	$1.6 \cdot 10^{-2}$; $1.3 \cdot 10^{-4}$; $1.6 \cdot 10^{-5}$; 0	
cwdmort	Mortality rate associated with CWD infection (F and PR; other seasons)	0.11; 0.32	Miller *et al.* (2008)
cwdsol	Probability of becoming solitary when clinical CWD starts	0.64	Mejia Salazar et al., 2016)
grmixed	Mixed group size (EG; PR and R)	8 – 11; 4 - 7	Mejia Salazar *et al.* (2016)
grdoe	Doe group size (EG; F, PR and R)	4 – 6; 2 - 5;	Mejia Salazar *et al.* (2016)
grbuck	Buck group size (LG; F)	3 – 6; 3 - 4	Mejia Salazar *et al.* (2016)
gryearling	Yearling group size (F)	2 - 4	Mejia Salazar *et al.* (2016)
disp	Probability for a yearling to disperse (male; female)	0.6; 0.35	Robinette (1966)
disprange	Max. number of cells a deer can move for dispersion	4	Hamlin and Mackie (1989)
migrrange	Max. number of cells a deer can move for migration	10	Mackie (1998)
speed	Displacement speed (in km/day)	16	Lendrum *et al.* (2013)

Table S4. Epidemiological parameters employed for the modelling.

Parameter	Description	Value	Source
β	Within group transmission rate	0.85	Jennelle *et al.* (2014); Potapov *et al.* (2013)
β'	Environmental transmission rate	2·10-4	Jennelle et al. (2014)
β_c	Probability of transmission from carcass given a contact	0.037	Miller *et al.* (2004)
λ, λ_G, λ_E, λ_C	Probability of being infected each step (total; from group; from environment; from carcass)	Eq. 9-16	Based on Jennelle *et al.* (2009); Potapov *et al.* (2013)
δ_{ff}, δ_{fm}, δ_{mf}, δ_{mm}	Interaction rate (female-female; female-male; male-female; male-male)	0.52; 1.04; 0.52; 1.91	Mejia Salazar (2017)
φ_f, φ_m, φ_{fa}	Food consumption rate (female, male, fawn)	0.93; 0.88; 1.19	Potapov *et al.* (2013)
ρ	Probability of visiting a carcass each step	$1.6 \cdot 10^{-4}$	Numerically optimized from Jennelle *et al.* (2009)
I_{fgr}, I_{mgr}, I_{fagr}	Number of infected deer within the group (females, males, fawns)		Model output
$I_{365cell}$	Number of infected deer that have been in the grid cell in the last 365 days		Model output
N_{fgr}, N_{mgr}, N_{fagr}	Number of deer within the group (females, males, fawns)		Model output
$N_{carcass}$	Number of carcasses in the grid cell		Model output
τ	Days of carcass persistence in the environment	Eq. 6-8	Numerically optimized from Jennelle *et al.* (2009)
d_i	Number of days an infected deer *i* has spent in the grid cell		Model output
βdif	Probability of CWD diffusion to a neighboring cell	Eq. 17	Model output

The California Department of Fish and Wildlife (CDFW) provided the proportional distribution of mule deer across spatial cells (CDFW, unpublished data). The initial mule deer abundance in the model (N) was calculated by multiplying this proportion by a statewide population estimate, allowing the total abundance to be adjusted for computational efficiency and enabling exploration of different overall deer density scenarios while preserving the underlying spatial pattern of relative distribution. The type of range for each cell (summer range, winter range, or year-round range) was also provided by the CDFW (see Figure S1). The *K* was considered to be associated with the habitat suitability (Muñoz *et al.* 2015). Therefore, a habitat suitability (*hs*) value for each cell was calculated from land cover based on the Stanke *et al.* (2018) classification. Given the set of grid cells

205 *n*, which comprises the overall state of California, the *K* of a given grid cell *i* was calculated by considering the
206 maximum *N* of the set of cells *n* and the habitat suitability (*hs*) as follows:

$$K_i = hs_i \cdot \max\{N_n\} \quad (1)$$

207 The CDFW provided data on migratory corridors based on animals collared with GPS transmitters in
208 various populations across the state. These data classified the areas used as migratory corridors by each
209 population into three categories: standard (used by between 0 and 10% of the marked animals in that population),
210 moderate (between 10 and 20%), and high use (more than 20%). We assigned to these areas the coefficients 1.1,
211 1.2 and 1.3, respectively, while the remaining portion of the State was assigned a value of 1. For each grid cell,
212 we pondered the values by surface to obtain a parameter of use as migratory corridor (*corr*). This parameter was
213 then combined with the *hs* parameter and the average terrain slope (*slope*) to assign a resistance value to each
214 cell (state variable *weight*) using the following formula:

$$weight_i = (1 - hf_i) \cdot 50 + {slope_i}/{corr_i} \quad (2)$$

215 A *weight* value ranging from 0 to 100 is obtained for each cell. The higher the *weight*, the greater the
216 resistance of the cell to the movement and residence of the mule deer. The objective of this approach is to
217 encourage the majority of the deer to migrate along the same cells, thereby forming migratory corridors
218 (Monteith *et al.* 2018), and to aggregate them in the most favorable areas during the winter months (D'Eon &
219 Serrouya 2005).

220 **Table S5.** Drought and wildfire related parameters employed in the model.

Parameter	Description	Value	Source
droughtp	Drought probability each year	0.2	Mount, Escriva-Bou and Sencan (2021)
firep	Wildfire probability in a given cell each year	0.015	Numerically optimized from CALFIRE data
bigfirep	Probability for a wildfire of burning the neighboring cells	0.0028	Numerically optimized from CALFIRE data

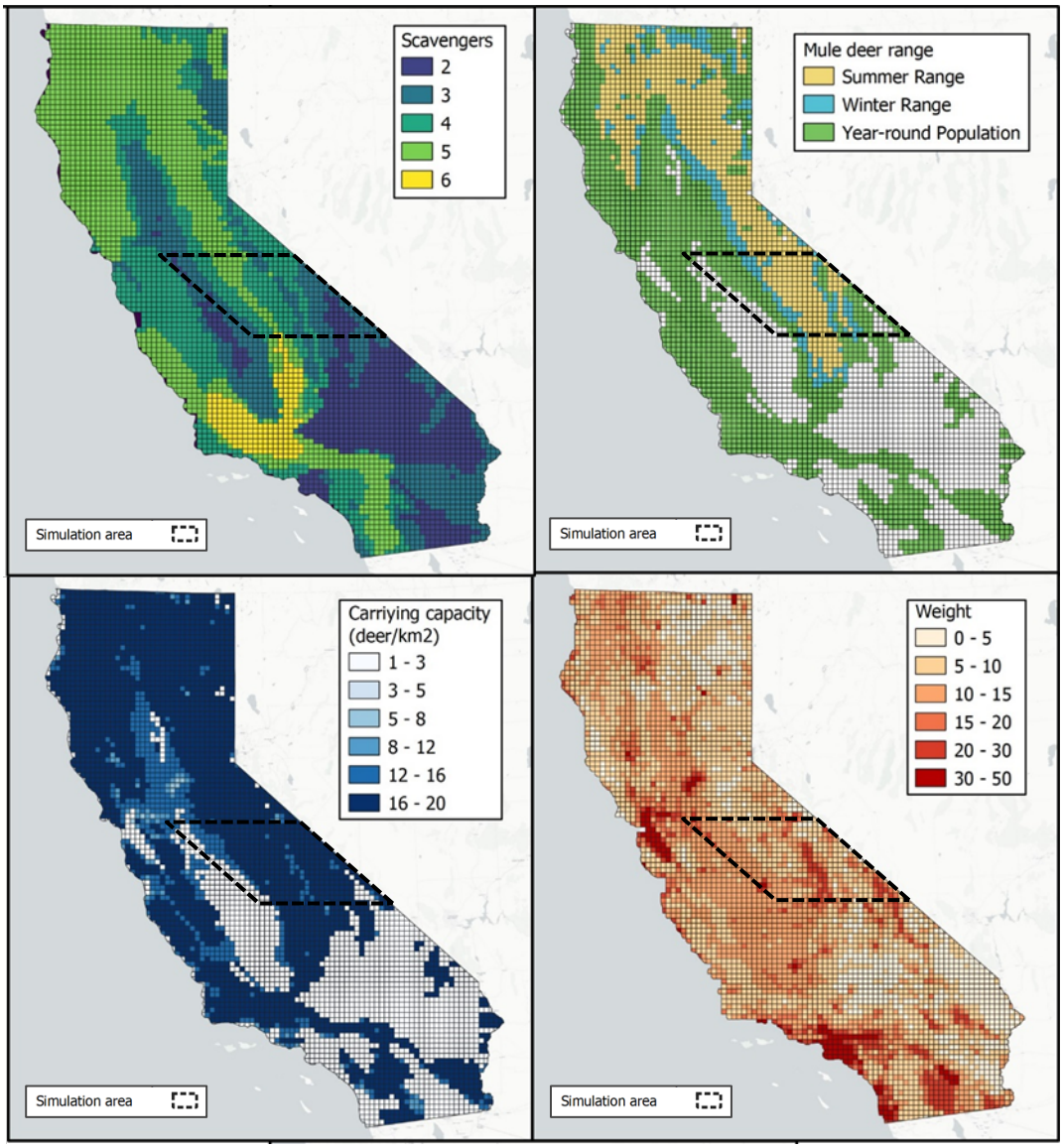

Figure S1. Initial values of the state variables of the grid cell agents utilized in the simulation, with the black-dashed line representing the boundaries of the simulation area.

1.6 Input data

The model does not use input data to represent time varying processes.

1.7 Submodels

1.7.1 Aging

Every step each deer agent increases the *age* value by 1 day. The state variable *class* changes from 1 (fawns) to 2 (yearlings) when *age* = 366 days (1 year), to 3 (adult) when *age* = 731 days (2 years), and to 4 (old) when *age* = 3286 days (9 years) for males and *age* = 4016 days (11 years) for females.

1.7.2 Natural mortality

Natural mortality occurs every step. The survival of fawns during the winter months was considered to be affected by starvation in cases where the abundance of deer is higher than the 85% of the *K* (Bergman *et al.* 2015). We employed a simple survival to starvation index (*starv*) based on Potapov *et al.* (2013):

$$starv = \min\left\{1,\quad 0.85 \cdot {K}/{N}\right\} \tag{3}$$

Consequently, the survival rate of yearlings and adults is determined by the *surv* parameter. For fawns, it results from the product of *fawnsurv* and *starv* parameters. For old deer, it is estimated as a linear decline from the *surv* value to 0 at the maximum age (Gross & Miller 2001), resulting in the following equations for males and females, respectively:

$$oldsurv_m = -0.29 \cdot {age}/{365} - 3.4 \tag{4}$$

$$oldsurv_f = -0.17 \cdot {age}/{365} - 2.72 \tag{5}$$

1.7.3 Hunting mortality

Hunting mortality occurs every step during the hunting season. The hunting pressure is calculated for each cell, age group, and sex at the beginning of each hunting season. The probability of an individual being hunted during the season is obtained by randomly sampling from a gamma distribution Γ (k_{hunt}, θ_{hunt}). This probability is then divided over the 85 days of the hunting season to obtain the probability of being hunted at each step.

1.7.4 CWD mortality

Miller *et al.* (2008) observed that deer infected with CWD were more susceptible to death from causes not directly related to the disease, such as hypothermia or predation. In their study, the diagnosis of CWD was performed using immunohistochemical staining, which allows for the preclinical detection of CWD in mule deer between 6 and 12 months after infection (Haley *et al.* 2012). Given that prion shedding commences 6-9 post-infection (Plummer *et al.* 2017; Tamguney *et al.* 2009), we considered an increase of *cwdmort* in mortality for infectious deer. All infected deer die 504 to 610 days after infection (Johnson *et al.* 2011; Williams 2005).

1.7.5 Carcass removal

When a deer infected with CWD dies, its carcass remains infectious in the environment until it decomposes or is consumed as carrion (Miller *et al.* 2004). Jennelle *et al.* (2009) assessed the persistence of deer carcasses in the environment concluding that season and scavenging pressure are the primary determinants. We used the data collected in their research to estimate de carcass survival (τ) for the four scheduled seasons considering the number of main scavenger species present (*scvg*;):

$$\tau_{PR\ and\ R} = 33.78^{-0.27 \cdot scvg} \quad (6)$$

$$\tau_{EG} = 63.24^{-0.06 \cdot scvg} \quad (7)$$

$$\tau_{LG\ and\ F} = 71.21^{-0.24 \cdot scvg} \quad (8)$$

Black bear (*Ursus americanus*), mountain lion (*Puma concolor*), coyote (*Canis latrans*), California condor (*Gymnogyps californianus*), turkey vulture (*Cathartes aura*), and the feral pig (*Sus scrofa*) were considered as potential scavengers of mule deer carcasses (Allen *et al.* 2015; 2021; Bauer *et al.* 2005; Jennelle *et al.* 2009). The information about the presence of these species was provided by the CDFW.

1.7.6 Fawning

During EG season, each female deer older than 548 days (1.5 years) has *preg* probability of fawning. In case of fawning, it has *twinp* probability of giving birth to twins. Sex ratio at birth is determined by the *fawnsex* parameter.

1.7.7 Group dynamics

During PR and R periods, females without fawns are in groups of size *grdoe,* and males are in mixed groups of size *grmixed* with females and fawns. At the beginning of EG, small doe groups and mixed groups join together to form larger groups of sizes *grdoe* and *grmixed,* respectively. In LG period, adult and old males leave the mixed groups to form male groups of size *grbuck*. During F season, pregnant females separate and give birth, forming groups with their fawns. Yearlings separate and form their own groups of size *gryearling*. When the yearly cycle comes to an end and the PR period begins again, male and yearling groups join females with fawns forming mixed groups of size *grmixed,* and females without fawns remain in groups of size *grdoe.*

1.7.8 Dispersal

When the time comes for dispersal, each yearling deer has *disp* probability for dispersion. If $N \geq 0.7 \cdot K$ in the grid cell where the deer is located, the probability of dispersal is 1. When a deer disperses, it moves to the nearest grid cell in which $N \leq 0.7 \cdot K$ in a *disprange* range of cells around its starting grid cell. Cells outside the summer or year-round range are discarded. If there are no cells in *disprange* that meet the aforementioned conditions, the deer will move to the cell with the least *weight* in *disprange*. Movements were assumed to follow the principle of least effort (Zipf 1949), which means that displacements occur through the cells with a lower *weight* value. The speed of movement is determined by the *speed* parameter.

1.7.9 Migration

As the fall migration period begins, all migratory deer move from their cells in the summer range to a randomly selected cell in the winter range that meets $N \leq 0.8 \cdot K$ within a *migrrange* range of cells around its starting grid cell. Therefore, they do not necessarily migrate to the same area every year (van de Kerk *et al.* 2021). Migrations occur in groups (Shellard & Mayor 2020), with all deer belonging to the same group migrating to the same cell. If there are no cells in a *migrrange* distance that meet this condition, the deer will move to the cell with the least *weight* in the winter range in a the *migrrange* range of cells. In spring migration, all migratory deer moves from its cell in the winter range to the cell where it was located before fall migration. Displacements occur through the cells with the lower *weight* values at a speed determined by the *speed* parameter.

1.7.10 Carrying capacity dispersal

The model assumes that when $N > 0.9 \cdot K$ in a cell, a dispersal process begins as a result of intraspecific competition for available resources (Valente *et al.* 2020). In a cell where this condition is met, the probability of a deer leaving the cell at each step (P_k) is determined as follows:

$$P_k = {0.1 \cdot (N - 0.9 \cdot K)}/{0.9 \cdot K} \quad (9)$$

This process causes the population to fluctuate slightly around the *K* of the cell. When a deer leaves the cell, it moves to the nearest grid cell where $N \leq 0.7 \cdot K$ in a *disprange* range of cells around its starting grid cell. The target cell must belong to the same seasonal range as the starting cell (summer or winter) or be a year-round range cell. If there are no cells in *disprange* that meet these conditions, it moves to the cell with the least *weight*

in *disprange*. The deer move through the cells with the lower *weight* value at a speed determined by the *speed* parameter.

1.7.11 CWD Force of infection

CWD transmission may be frequency-dependent (FD) density-dependent (DD), or a combination of both (Grear *et al.* 2010; Jennelle *et al.* 2014; Storm *et al.* 2013; Winter & Escobar 2020). FD within-group transmission is considered to be the main mechanism of CWD transmission (Potapov *et al.* 2013; 2016; Storm *et al.* 2013). However, intergroup environmental transmission, which is a DD mechanism, has been shown to play a role in the disease dynamics, especially after a long period of time when the disease becomes endemic (Almberg *et al.* 2011; Miller, Hobbs & Tavener 2006). Therefore, we considered both within-group transmission and environmental transmission between groups, excluding FD transmission between groups since direct contacts between groups are rare and the likelihood of infection from a single contact is low (Belsare & Stewart 2020; Habib *et al.* 2011; Kjaer 2010). We also considered the possibility of transmission from an infectious carcass (Miller *et al.* 2004). Thus, the probability of becoming infected at each step for a given individual is determined by the probability of becoming infected by another individual of the same group (λ_G), the probability of becoming infected by the environment (λ_E), and the probability of becoming infected by an infectious carcass (λ_C).

1.7.11.1 Transmission rates (β and β´)

Actual values of transmission rates for mule deer in California are not available, although estimates have been made for other populations and species have been carried out (Almberg *et al.* 2011; Jennelle *et al.* 2014; Miller, Hobbs & Tavener 2006; Potapov *et al.* 2016; Wasserberg *et al.* 2009). CWD prevalence rates in males can be up to twice as high as in females, and lower in yearlings (Edmunds *et al.* 2016; Heisey *et al.* 2010; Osnas *et al.* 2009), leading Jennelle *et al.* (2014) to suggest a different transmission rate for males and females as the most plausible option in their study of white-tailed deer (*Odocoileus virginianus*). However, higher prevalence in males and adults is likely associated with consumption and interaction behavior (Potapov *et al.* 2013), which may vary between species. Consequently, we decided to use sex-independent transmission rates of $\beta = 0.85$ infections·year^{-1} (Jennelle *et al.* 2014; Potapov *et al.* 2016) for within-group transmission and β´ =

$2 \cdot 10^{-4}$ infections·year^{-1}·individual^{-1} (Jennelle *et al.* 2014) for environmental transmission, and combine them with parameters related to food consumption and interaction rates.

1.7.11.2 Probability of group infection (λ_G)

For the within-group transmission, we included a parameter related to interaction rates (δ), with higher values assigned to males than to females and fawns (Mejia Salazar 2017). The probability of an individual being infected by a group member each time step for females (*f*), males (*m*) and fawns (*fa*) is calculated as follows:

$$\lambda_{Gf} = {}^{\beta}/_{365} \cdot \delta_{mf} \cdot \frac{I_{mgr}}{N_{mgr}} + {}^{\beta}/_{365} \cdot \delta_{ff} \cdot \frac{I_{fgr} + I_{fagr}}{N_{fgr} + N_{fagr}} \quad (10)$$

$$\lambda_{Gm} = {}^{\beta}/_{365} \cdot \delta_{mm} \cdot \frac{I_{mgr}}{N_{mgr}} + {}^{\beta}/_{365} \cdot \delta_{fm} \cdot \frac{I_{fgr} + I_{fagr}}{N_{fgr} + N_{fagr}} \quad (11)$$

$$\lambda_{Gfa} = {}^{\beta}/_{365} \cdot \delta_{mf} \cdot \frac{I_{mgr}}{N_{mgr}} + {}^{\beta}/_{365} \cdot \delta_{ff} \cdot \frac{I_{fgr} + I_{fagr}}{N_{fgr} + N_{fagr}} \quad (12)$$

1.7.11.3 Probability of environmental infection (λ_E)

Although CWD prion can be found in the soil and plants for a long time after excretion (Mathiason *et al.* 2009; Miller *et al.* 2004; Plummer *et al.* 2018), Miller *et al.* (2004) reported a rapid rate of removal of the amount of prions from the environment. Potapov *et al.* (2013) evaluated the impact of infected deer in the past, concluding that the effect is weak and justifying the assumption of one year of pathogen survival in the environment. Consequently, we calculated the probability of infection from an environmental source of prions for a given deer at each step considering the sum of days that every excreting deer spent in the grid cell during the previous 365 days. A food parameter related to food consumption (φ) was also included:

$$\lambda_{Gf} = {}^{\beta'}/_{365} \cdot \varphi_f \cdot \sum_{i=1}^{I_{365cell}} d_i \quad (13)$$

$$\lambda_{Gm} = {}^{\beta'}/_{365} \cdot \varphi_f \cdot \sum_{i=1}^{I_{365cell}} d_i \quad (14)$$

$$\lambda_{Gfa} = {}^{\beta'}/_{365} \cdot \varphi_{fa} \cdot \sum_{i=1}^{I_{gridcell-365\ days}} d_i \quad (15)$$

1.7.11.4 Probability of carcass infection (λ_C)

The transmission from infectious deer carcasses to healthy deer has already been proven (Miller *et al.* 2004). Furthermore, the nutrient supply from the carcass to the soil leads to an increase in vegetation, entailing attraction effect for ungulates (Towne 2000; Walker *et al.* 2020). However, transmission from carcasses is usually overlooked in CWD epidemiological studies. We used the data collected by Jennelle *et al.* (2009) to estimate the probability of a given deer in a cell visiting a carcass at each step (ρ), which was then combined with the probability of infection through contact with a carcass (β_C) estimated by Miller *et al.* (2004). Consequently, the probability of infection by a carcass present in the grid cell at each step can be estimated. When combined with the number of carcasses present in the grid cell ($N_{carcass}$), this leads to the probability of infection from carcasses at each step.

$$\lambda_C = \beta_C \cdot \rho \cdot N_{carcass} \tag{16}$$

1.7.12 CWD Diffusion

The discretization of space into a grid signifies that the only way an individual in a cell other than the outbreak cell can become infected is through the arrival of an infected individual, either by dispersal or migration. Since individuals at the edge of a cell could come into contact and form groups with individuals from neighboring cells, thereby spreading the pathogen, a diffusion model is also added to the simulation. The spread rate is typically between 5 and 10 km per year from a focus of all infected individuals (Garlick *et al.* 2014; Xu, Merrill & Lewis 2022). In our grid, this would imply that from a cell where all individuals are infected, all 8 neighboring cells would also be infected within a year. The lower the prevalence, the lower the probability of neighboring cells becoming infected. For the diffusion model, we assume that the relationship between prevalence and the probability of diffusion is linear. Xu, Merrill and Lewis (2022) observed a correlation between the density of deer groups and the speed of spread, since a higher number of groups increases the likelihood of contact between them. Based on their calculations, we assumed that there is a linear relationship between the speed of expansion and the density of deer groups present, from 1.5 km/year (which would take approximately 5 years to spread to neighboring cells) for 1 group per 100 km², to 7.5 km/year (which would take approximately 1 year) for 100 groups per 100 km². Consequently, for each infected cell *i* (i.e., with at least

one infected individual) with *Ngr* deer groups inside, the probability (*βdif*) of an individual in a neighboring cell *z* becoming infected at each step is calculated as follows:

$$\beta dif_z = prevalence_i \cdot (0.2 + 0.008 \cdot Ngr_i)/365 \quad (17)$$

1.7.13 Droughts

Every year there is a probability *droughtp* that an interannual drought will begin, lasting between 365 and 1460 days (1 to 4 years; Miller *et al.* 2022). The drought covers the entire State of California resulting in an increase in mortality rates by 15% (Jackson *et al.* 2021; Schuyler, Dugger & Jackson 2018) and in the probability of wildfires by 40% (Littell *et al.* 2016; Madadgar *et al.* 2020). Furthermore, a 25% reduction in *K* is also considered.

1.7.14 Wildfires

Each cell has a probability *firep* of undergoing a wildfire during the summer. Similarly, each wildfire has a probability *bigfirep* of spreading the wildfire to the neighboring cells. When a cell burns out, it is assumed that the environmental prion load is removed by high temperatures (Lee 2023), signifying that $\sum_{i=1}^{I_{365cell}} d_i = 0$ (see Equations 13-15).

Furthermore, an effect on *K* of the cell is considered (Bristow *et al.* 2020; Sparks *et al.* 2018). This effect is observed to decrease to a minimum during the first year after the fire (5%), increase over the second year due to the growth of low vegetation (190%), and stabilize from the third and fourth years (90%) before returning to its original value from the fifth year after the wildfire. The substantial reduction in *K* due to a fire initiates a dispersion process (see Equation 9), in which a large difference between *N* and *K* would result in the vast majority of deer in the cell fleeing ahead in a very short time (van Mantgem, Keeley & Witter 2015).

Appendix 2: Model evaluation

The ecological module of the model was evaluated through long-term population trends. In California, mule deer populations have been slightly declining for several decades (Loft & Bleich 2014; Webb 2013). To ensure that this pattern was reflected in the model, 20 iterations were conducted over a simulation of 50 years (18,250 steps) with a population of 10,000 deer in an area of 41,000 km^2 covering all mule deer ranges (summer, winter and year-round). These simulations were performed without initiating CWD outbreaks, in order to assess the population dynamics in the absence of the pathogen. The simulations showed a slight decline in the mule deer population over a 50-year period, with an average abundance of 8,370 individuals across the 20 iterations (ranging from 6,326 to 11,166) at the end of the simulation (see Figure S2). This outcome aligns with the observed population pattern of mule deer in California over the past few decades (Loft & Bleich 2014; Webb 2013).

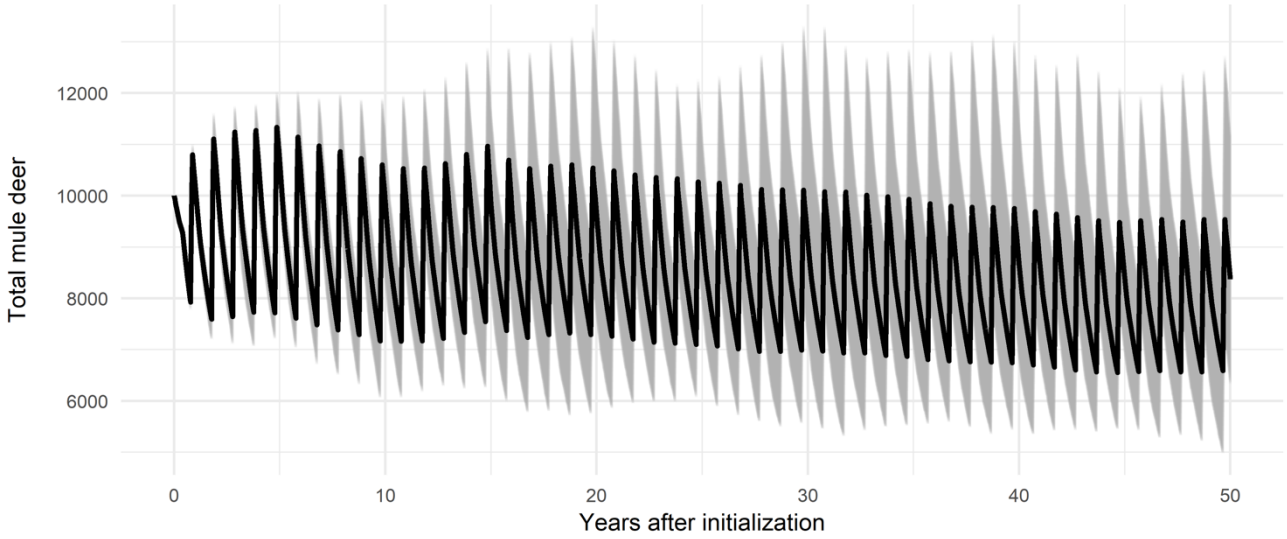

Figure S2. Evolution of the total number of mule deer over a 50-year simulation. The initial population was 10,000 deer in an area of 41,000 km². The black line represents the average value across 20 iterations, while the gray shading represents the maximum and minimum values.

The epidemiological module is more challenging to evaluate due to the lack of empirical data on the prevalence and distribution of the disease in California. Observed patterns in CWD dynamics indicate a higher prevalence in bucks (adult and old males) than in does (adult and old females) and yearlings (Edmunds *et al.* 2016; Grear *et al.* 2006; Miller & Conner 2005; Osnas *et al.* 2009) and a spread velocity between 3.7 and 11

km/year (Garlick *et al.* 2014; Xu, Merrill & Lewis 2022). Consequently, the model's results were evaluated through these patterns. To this end, 5 iterations of simulations lasting 7 years and 9 months (2,828 steps) were conducted, with an initial modeled population of 46,160 mule deer, assumption based on publicly reported statewide population estimates of 500,000–1,000,000 deer (WAFWA, 2025) and distributed across a 41,000 km^2 of simulation landscape according to the proportional distribution. The outbreaks were initiated on May 1st, as this is the month when the first cases have been detected (Munk & Benedet 2024). This is 9 months after the start of the simulation on August 1st, signifying 7 years of pathogen spread simulation. The outbreaks were initiated in a non-migratory population to avoid the potential impact of migratory movements on the spatial dynamics of the pathogen, since such movements could influence the spread rate or prevalence rates.

Table S6. Accumulated exposed mule deer and CWD prevalences by sex and age class over 7 years of pathogen presence in an initial population of 46,160 mule deer in an area of 41,000 km², with the outbreak initiating in a non-migratory population. The values at the end of the simulation are shown for the 5 iterations.

Iteration	Accumulated exposed mule deer	Prevalence rates (whole simulation area)			
		Bucks	Does	Yearlings	Fawns
1	2,884	4.48 %	4.81 %	3.78 %	4.78 %
2	2,890	8.71 %	8.52 %	7.87 %	9.76 %
3	2,143	7.88 %	6.29 %	5.71 %	7.23 %
4	2,171	3.54 %	3.20 %	2.77 %	3.91 %
5	2,289	5.75 %	4.99 %	4.62 %	5.98 %

As a result, CWD exhibited an average spread of 50 km across the 10 iterations (ranging from 48 to 53 km) over the 7 years, resulting in an average spread rate of 7.1 km/year (ranging from 6.9 to 7.6 km/year). This value is consistent with the expected rates observed in previous studies (3.7 to 11 km/year in Garlick *et al.* 2014; 7.3 km/year in Xu, Merrill & Lewis 2022). The prevalence of CWD was found to be higher in bucks than in does and yearlings in all iterations, with a the exception of one iteration where the prevalence in does was slightly higher (4.81% compared to 4.48%, see Table S6), as expected by previously reported values (Edmunds *et al.* 2016; Grear *et al.* 2006; Miller & Conner 2005). The prevalence of CWD in fawns was indeed higher than expected based on previously reported values (Heisey *et al.* 2010; Osnas *et al.* 2009). However, the few data regarding prevalence rates in fawns pertain to populations of a different species (white-tailed deer) in areas where CWD is endemic, and the disease dynamics may differ.

Therefore, the demographic patterns of mule deer populations and the epidemiological patterns of CWD are shown to be within the expected range based on previous observational studies. Thus, the model's parameterization is shown to be reliable, lending credibility to the potential emergence of spatiotemporal patterns derived from the model.

Appendix 3: Parameter optimization

Some of the parameters included in the modeling were estimated based on information derived from previous scientific research and reports published by the California Department of Fish and Wildlife (CDFW) and the California Department of Forestry and Fire Protection (CALFIRE). This appendix provides an account of the processes employed to obtain these parameters.

3.1. Hunting pressure (k_{hunt}, θ_{hunt})

Hunting pressure was estimated based on mule deer population estimates and hunting statistics reports from CDFW. These reports are publicly available at https://wildlife.ca.gov/Conservation/Mammals/Deer/Population and https://wildlife.ca.gov/Hunting/Deer, respectively. In order to ascertain the distribution of hunting pressure by age and sex classes, the percentage of hunted mule deer corresponding to male yearlings, adult/old females (does), and adult/old males (bucks) was calculated based on the data included in the hunting statistics reports which included the information categorized by sex and age class, spanning from 2013 to 2017 (see Table S7).

Table S7. Hunting statistics for the entire state of California by sex and age class between the years 2013 and 2017.

Year	% Yearling males	% Does	% Males
2013	0.1	2.2	97.6
2014	0.1	2.0	97.9
2015	0.1	1.7	98.2
2016	0.1	1.6	98.3
2017	0.1	1.8	98.1
Average	0.1	1.9	98.0

The proportion of the mule deer population in each hunting area was derived from statewide abundance estimates of 500,000–1,000,000 deer (WAFWA, 2025) and the proportional distribution provided by CDFW (unpublished data). Sex- and age-class abundances (male yearlings, does, and adult bucks) were estimated using the proportions in Table S8 of the ODD protocol. Hunting pressure within each area was then calculated by multiplying the total number of individuals harvested by the proportional distribution and dividing this value by the abundance of the corresponding sex and age class (see Table S8). A Gamma distribution Γ (k, θ) was employed to fit the hunting pressure for each sex and age class (see Figure S1). The hunting pressure in each

cell is calculated annually by sampling from each of these Gamma distributions, thereby introducing spatial and temporal stochasticity to the hunting pressure. The increases in mortality of old and adult male deer resulting from the calculated hunting pressure are consistent with data derived from studies conducted in other areas (Bishop *et al.* 2005; Forrester & Wittmer 2013).

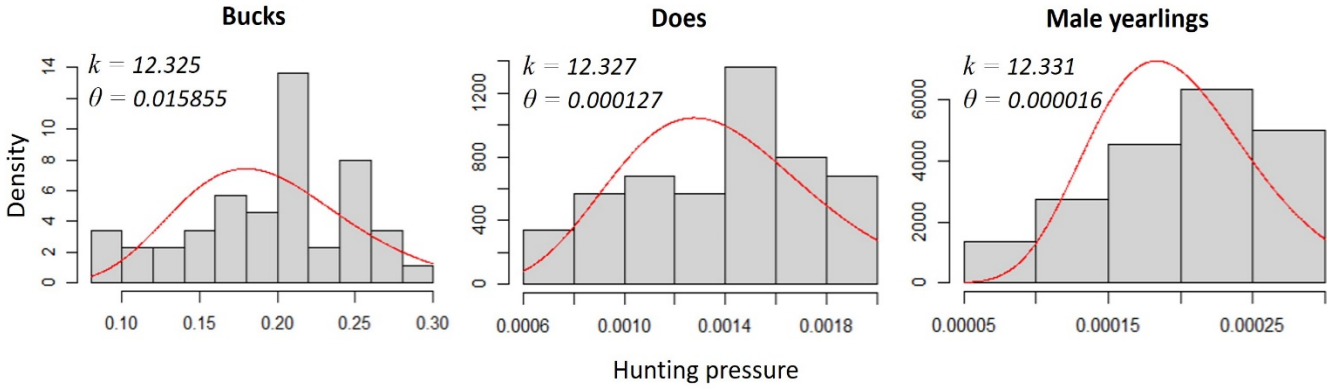

Figure S1. Gamma fitting to the mule deer hunting pressure values from the different game management areas of California.

3.2. Probability of visiting a carcass (ρ)

Jennelle *et al.* (2009) observed an average of 0.24 visits per day by white-tailed deer (*Odocoileus virginianus*) to carcasses of the same species. The study was conducted in an area of 544 km², with a mean deer density of 14.5 individuals per km². This would signify an approximate abundance of 7,888 deer throughout their study area. Given the aforementioned visit frequency, the probability of each deer visiting a single carcass in 544 km2 would be 0.24/7888 = 3.10-5. If the carcass were located in the more restricted space of 100 km^2 by a cell of the grid utilized in the model, the probability would be $\rho = 3 \cdot 10^{-5} \cdot 544/100 = 1.6 \cdot 10^{-4}$.

3.3. Carcass duration in the environment (τ)

In the same study, Jennelle et al. (2009) evaluated the persistence of deer carcasses in the environment, concluding that season and scavenging pressure are the primary determinants. To estimate the persistence of carcasses (τ) for the four scheduled seasons, we fitted an exponential regression to the data collected in their research in each season (see Figure S2):

$$\tau_{PR\ and\ R} = 33.78^{-0.27 \cdot scvg}$$

$$\tau_{EG} = 63.24^{-0.06 \cdot scvg}$$

$$\tau_{LG\ and\ F} = 71.21^{-0.24 \cdot scvg}$$

Where *PR* is the pre-rut period, *R* is the rut period, *EG* is the early gestation period, *LG* is the late gestation period, *F* is the fawning period, and *scvg* is the number of scavenging species present.

Table S8. Hunting statistics for each mule deer game management area in California.

Hunting Zone	Hunting pressure bucks	Hunting pressure Does	Hunting pressure male yearlings
A	0.2313560	0.0016447	0.0002361
B1	0.2507064	0.0017822	0.0002558
B2	0.2812340	0.0019992	0.0002870
B3	0.2580933	0.0018347	0.0002634
B4	0.2468463	0.0017548	0.0002519
B5	0.2477257	0.0017610	0.0002528
B6	0.2690059	0.0019123	0.0002745
C1	0.1726837	0.0012276	0.0001762
C2	0.2493943	0.0017729	0.0002545
C3	0.2503392	0.0017796	0.0002554
C4	0.1193453	0.0008484	0.0001218
D3	0.2148399	0.0015273	0.0002192
D4	0.2015636	0.0014329	0.0002057
D5	0.2114740	0.0015033	0.0002158
D6	0.1835822	0.0013051	0.0001873
D7	0.1950312	0.0013864	0.0001990
D8	0.2280419	0.0016211	0.0002327
D9	0.1464952	0.0010414	0.0001495
D10	0.2130056	0.0015142	0.0002174
D11	0.2608757	0.0018545	0.0002662
D12	0.1518071	0.0010792	0.0001549
D13	0.2628537	0.0018686	0.0002682
D14	0.2577548	0.0018323	0.0002630
D15	0.0912905	0.0006490	0.0000932
D16	0.2046046	0.0014545	0.0002088
D17	0.1128264	0.0008021	0.0001151
D19	0.2131657	0.0015154	0.0002175
X1	0.2180585	0.0015501	0.0002225
X2	0.2064371	0.0014675	0.0002107
X3a	0.1882369	0.0013381	0.0001921

Hunting Zone	Hunting pressure bucks	Hunting pressure Does	Hunting pressure male yearlings
X3b	0.2011210	0.0014297	0.0002052
X4	0.2025321	0.0014398	0.0002067
X5a	0.1912099	0.0013593	0.0001951
X5b	0.1631488	0.0011598	0.0001665
X6a	0.2171950	0.0015440	0.0002216
X6b	0.1639525	0.0011655	0.0001673
X7a	0.1669881	0.0011871	0.0001704
X7b	0.1679218	0.0011937	0.0001713
X8	0.2067651	0.0014699	0.0002110
X9a	0.1238557	0.0008805	0.0001264
X9b	0.0887682	0.0006310	0.0000906
X9c	0.1405992	0.0009995	0.0001435
X10	0.0872043	0.0006199	0.0000890
X12	0.1385755	0.0009851	0.0001414

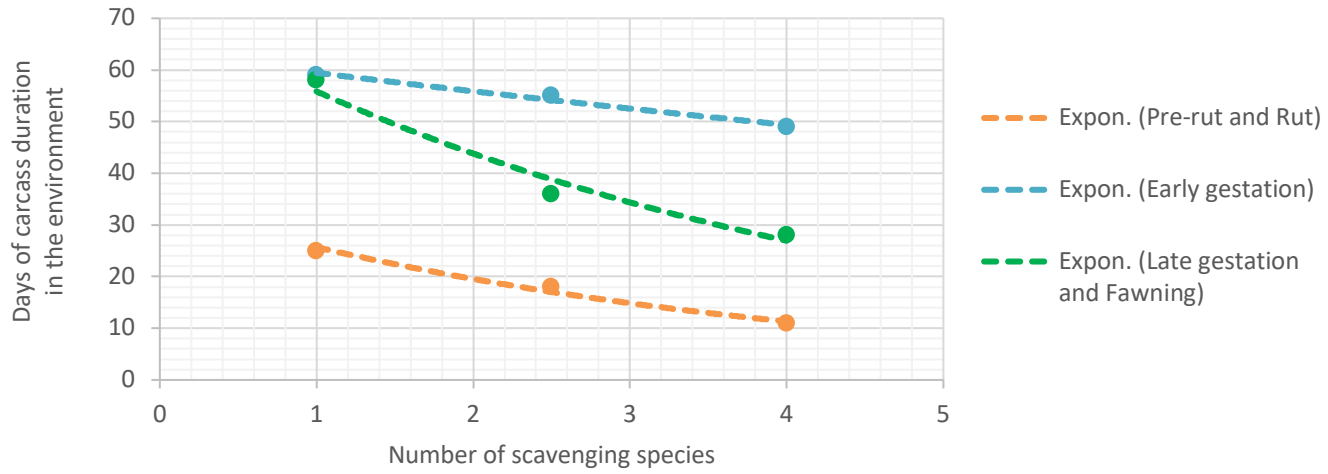

Figure S2. Exponential fitting to the data on carcass persistence in the environment collected by Jennelle *et al.* (2009).

The resulting persistence of a carcass in the environment for each season of the year and number of scavenging species included in the model is shown in Table S9.

Table S9. Duration of a deer carcass in the environment for each season and each number of scavenging species included in the model.

Number of scavenging species	Pre-rut and Rut	Early gestation	Late gestation and fawning
2	20	56	44
3	15	53	34
4	11	49	27
5	9	46	21
6	7	44	17

3.4. Wildfire and big fire probability (*firep and bigfirep*)

To estimate the probability of a cell burning each year (*firep*) and the probability that, given a fire, it becomes a large-scale fire (*bigfirep*), we utilized the CALFIRE incident database, which provides accurate information on fires that have occurred since 2013 to the present (available at https://www.fire.ca.gov/incidents). We excluded fires that burned an area smaller than 1 km² as they are not expected to have a significant effect on mule deer due to their mobility and home range (van Mantgem, Keeley & Witter 2015). The remaining fires with complete year information (from 2013 to 2023) were considered. The resulting total burned area was 43,215.5 km² over 11 years, signifying an average of 3,928.7 km² burned each year. Given that each grid cell has an area of 100 km², this would result in 3,928.7/100 = 393 cells burned each year. The majority of these fires occur within the mule deer distribution area in California (see Figure S3), which represents 25,580 cells in the grid used in the model. Consequently, if the number of cells expected to burn each year is divided by the total number of cells that can burn, a yearly fire probability in each cell is obtained, which is *firep* = 393/25,580 = 0.015.

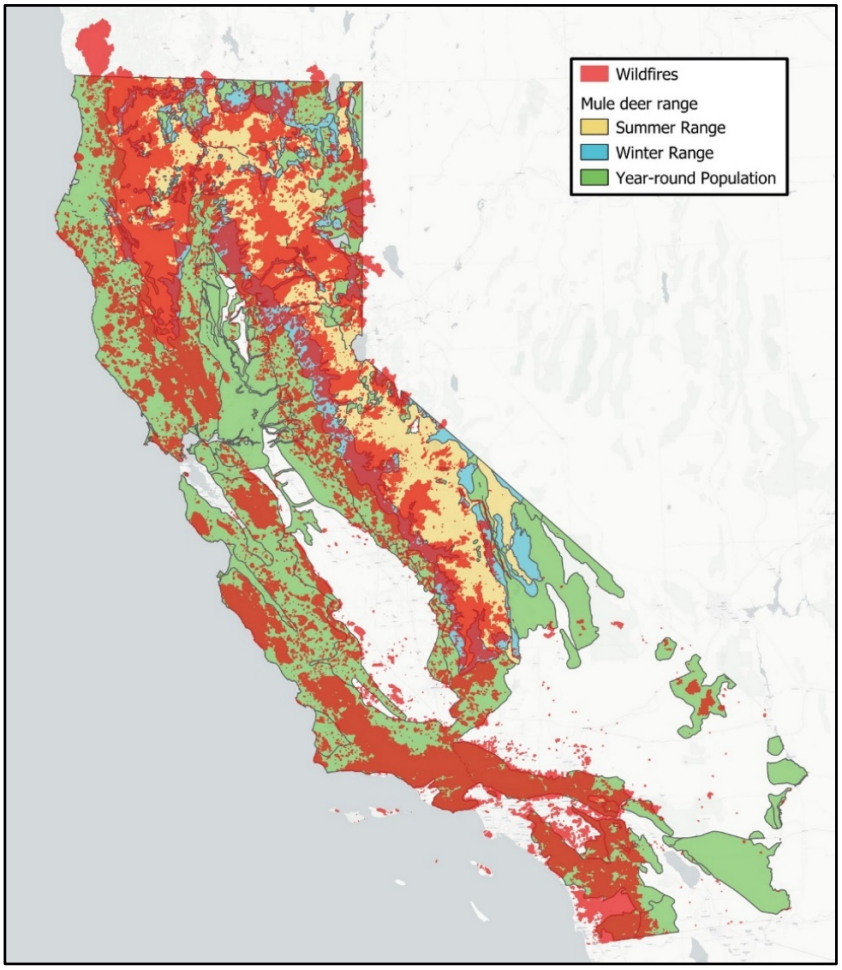

Figure S3. Area burned by historic wildfires in California, along with the distribution of mule deer. Compiled from data provided by CALFIRE and CDFW.

To calculate the probability of a fire becoming a large fire that burns the 8 neighboring cells (*bigfirep*), the number of fires larger than 800 km^2 (8 cells) was counted for the period from 2013 to 2023. A total of 12 fires were counted over 11 years, averaging 1.1 large fires per year. Given that 393 fires were calculated in cells each year, the probability of each of them becoming a large fire and burning the 8 neighboring cells would be *bigfirep* = 1.1/393 = 0.0028.

Appendix 4: Supplementary Figures

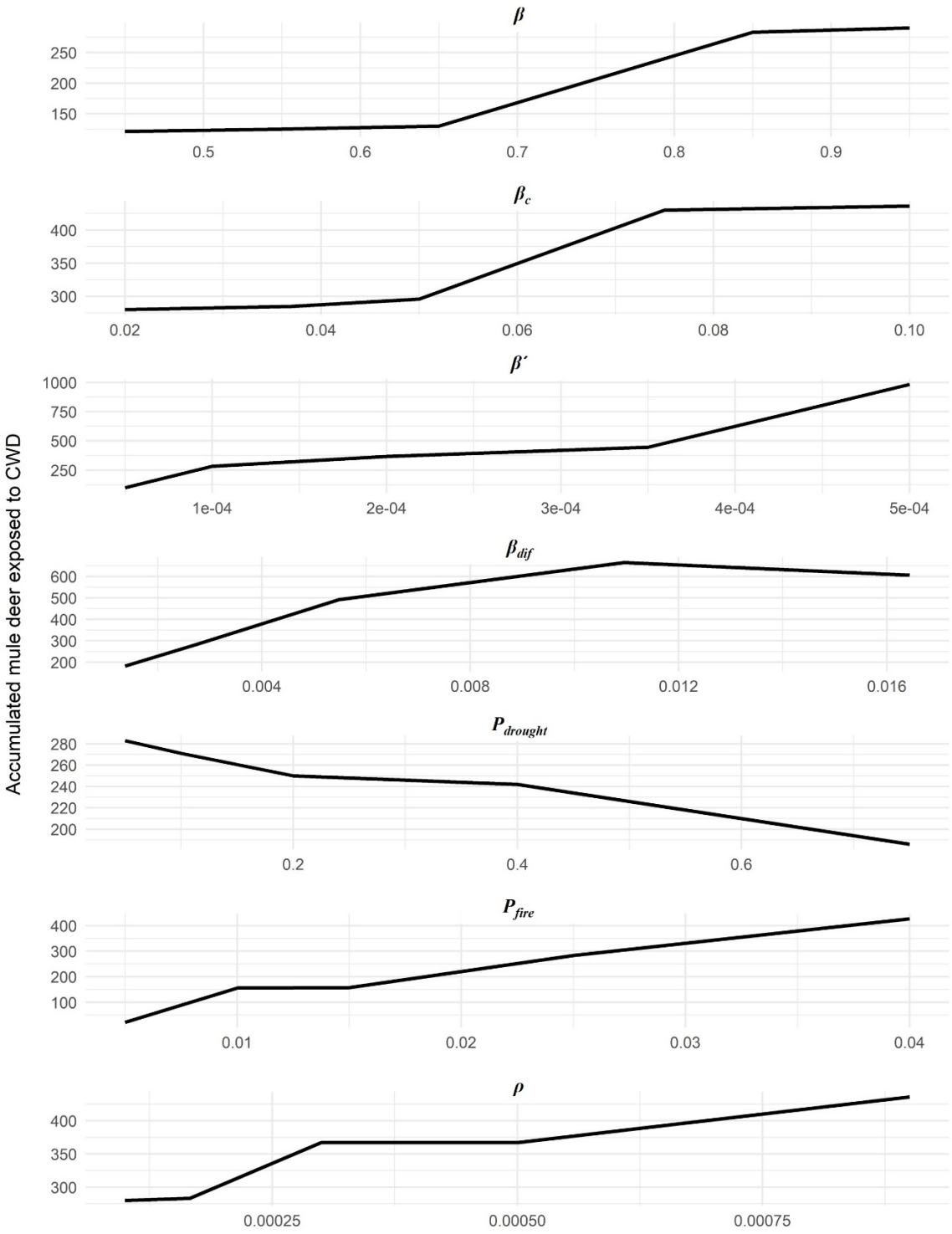

Figure S4. One-factor-at-a-time sensitivity analysis. The relationship between the output (the accumulated number of mule deer exposed to CWD at the end of the 7-year simulation following the CWD outbreak in an initial population of 10,000 mule deer) and the parameters is displayed. The following parameters were considered: within-group transmission rate (β), environmental transmission rate (β'), carcass transmission rate (β_c), diffusion rate (β_{dif}) probability of encountering a carcass (ρ), the probability of wildfires (P_{fire}) and the probability of drought ($P_{drought}$).

References

Ahlborn, G. & White, M. (2006) California Wildlife Habitat Relationships System: Mule Deer (*Odocoileus hemionus*). (ed. CDFW). California Interagency Wildlife Task Group, Sacramento.

Allen, M.L., Elbroch, L.M., Wilmers, C.C. & Wittmer, H.U. (2015) The comparative effects of large carnivores on the acquisition of carrion by scavengers. *Am Nat,* **185,** 822-833. 10.1086/681004

Allen, M.L., Elbroch, L.M. & Wittmer, H.U. (2021) Scavenging by fishers in relation to season and other scavengers. *Ecological Research,* **36,** 353-359. 10.1111/1440-1703.12198

Almberg, E.S., Cross, P.C., Johnson, C.J., Heisey, D.M. & Richards, B.J. (2011) Modeling routes of chronic wasting disease transmission: environmental prion persistence promotes deer population decline and extinction. *PLoS One,* **6,** e19896. 10.1371/journal.pone.0019896

Baeten, L.A., Powers, B.E., Jewell, J.E., Spraker, T.R. & Miller, M.W. (2007) A Natural Case of Chronic Wasting Disease in a Free-ranging Moose (Alces alces shirasi). *Journal of Wildlife Diseases,* **43,** 309-314. 10.7589/0090-3558-43.2.309

Bauer, J.W., Logan, K.A., Sweanor, L.L., Boyce, W.M. & Jones, C.A. (2005) Scavenging Behavior in Puma. *The Southwestern Naturalist,* **50,** 466-471. 10.1894/0038-4909(2005)050[0466:Sbip]2.0.Co;2

Belsare, A.V., Gompper, M.E., Keller, B., Sumners, J., Hansen, L. & Millspaugh, J.J. (2020) An agent-based framework for improving wildlife disease surveillance: A case study of chronic wasting disease in Missouri white-tailed deer. *Ecol Modell,* **417**. 10.1016/j.ecolmodel.2019.108919

Belsare, A.V. & Stewart, C.M. (2020) OvCWD: An agent-based modeling framework for informing chronic wasting disease management in white-tailed deer populations. *Ecological Solutions and Evidence,* **1**. 10.1002/2688-8319.12017

Bender, L.C. & Hoenes, B.D. (2018) Age-related fecundity of free-ranging mule deer *Odocoileus hemionus Cervidae* in south-central, New Mexico, USA. *Mammalia,* **82,** 124-132. 10.1515/mammalia-2016-0166

Benestad, S.L., Mitchell, G., Simmons, M., Ytrehus, B. & Vikøren, T. (2016) First case of chronic wasting disease in Europe in a Norwegian free-ranging reindeer. *Veterinary Research,* **47,** 88. 10.1186/s13567-016-0375-4

Bergman, E.J., Doherty, P.F., White, G.C. & Holland, A.A. (2015) Density dependence in mule deer: a review of evidence. *Wildlife Biology,* **21,** 18-29. 10.2981/wlb.00012

Bishop, C.J., Unsworth, J.W., Garton, E.O. & Ransom (2005) Mule Deer Survival among Adjacent Populations in Southwest Idaho. *Journal of Wildlife Management,* **69,** 311-321. 10.2193/0022-541x(2005)069<0311:Mdsaap>2.0.Co;2

Bishop, C.J., White, G.C., Freddy, D.J., Watkins, B.E. & Stephenson, T.R. (2010) Effect of Enhanced Nutrition on Mule Deer Population Rate of Change. *Wildlife Monographs,* **172,** 1-28. 10.2193/2008-107

Bristow, K.D., Harding, L.E., Lucas, R.W. & McCall, T.C. (2020) Influence of fire severity and vegetation treatments on mule deer (*Odocoileus hemionus*) winter habitat use on the Kaibab

Plateau, Arizona. *Animal Production Science,* **60,** 1292-1302. https://doi.org/10.1071/AN19373

California Department of Fish and Wildlife (2024) California's Deer Population Estimates [accessed 10/05/2024]. Available at https://wildlife.ca.gov/Conservation/Mammals/Deer/Population

D'Eon, R.G. & Serrouya, R. (2005) Mule Deer Seasonal Movements and Multiscale Resource Selection Using Global Positioning System Radiotelemetry. *Journal of Mammalogy,* **86,** 736-744. 10.1644/1545-1542(2005)086[0736:Mdsmam]2.0.Co;2

DeVivo, M.T., Edmunds, D.R., Kauffman, M.J., Schumaker, B.A., Binfet, J., Kreeger, T.J., Richards, B.J., Schatzl, H.M. & Cornish, T.E. (2017) Endemic chronic wasting disease causes mule deer population decline in Wyoming. *PLoS One,* **12,** e0186512. 10.1371/journal.pone.0186512

Diefenbach, D.R., Long, E.S., Rosenberry, C.S., Wallingford, B.D. & Smith, D.R. (2008) Modeling Distribution of Dispersal Distances in Male White-Tailed Deer. *Journal of Wildlife Management,* **72,** 1296-1303. 10.2193/2007-436

Edmunds, D.R., Kauffman, M.J., Schumaker, B.A., Lindzey, F.G., Cook, W.E., Kreeger, T.J., Grogan, R.G. & Cornish, T.E. (2016) Chronic Wasting Disease Drives Population Decline of White-Tailed Deer. *PLoS One,* **11,** e0161127. 10.1371/journal.pone.0161127

Escobar, L.E., Pritzkow, S., Winter, S.N., Grear, D.A., Kirchgessner, M.S., Dominguez-Villegas, E., Machado, G., Townsend Peterson, A. & Soto, C. (2020) The ecology of chronic wasting disease in wildlife. *Biol Rev Camb Philos Soc,* **95,** 393-408. 10.1111/brv.12568

Farnsworth, M.L., Hoeting, J.A., Hobbs, N.T. & Miller, M.W. (2006) Linking Chronic Wasting Disease To Mule Deer Movement Scales: A Hierarchical Bayesian Approach. *Ecological Applications,* **16,** 1026-1036. 10.1890/1051-0761(2006)016[1026:Lcwdtm]2.0.Co;2

Forrester, T.D. & Wittmer, H.U. (2013) A review of the population dynamics of mule deer and black-tailed deer *Odocoileus hemionus* in North America. *Mammal Review,* **43,** 292-308. 10.1111/mam.12002

Furnas, B.J., Landers, R.H., Hill, S., Itoga, S.S. & Sacks, B.N. (2018) Integrated modeling to estimate population size and composition of mule deer. *The Journal of Wildlife Management,* **82,** 1429-1441. 10.1002/jwmg.21507

Garlick, M.J., Powell, J.A., Hooten, M.B. & MacFarlane, L.R. (2014) Homogenization, sex, and differential motility predict spread of chronic wasting disease in mule deer in southern Utah. *J Math Biol,* **69,** 369-399. 10.1007/s00285-013-0709-z

Grear, D.A., Samuel, M.D., Langenberg, J.A. & Keane, D. (2006) Demographic Patterns and Harvest Vulnerability of Chronic Wasting Disease Infected White-Tailed Deer in Wisconsin. *Journal of Wildlife Management,* **70,** 546-553. 10.2193/0022-541x(2006)70[546:Dpahvo]2.0.Co;2

Grear, D.A., Samuel, M.D., Scribner, K.T., Weckworth, B.V. & Langenberg, J.A. (2010) Influence of genetic relatedness and spatial proximity on chronic wasting disease infection among female white-tailed deer. *Journal of Applied Ecology,* **47,** 532-540. 10.1111/j.1365-2664.2010.01813.x

Grimm, V., Berger, U., DeAngelis, D.L., Polhill, J.G., Giske, J. & Railsback, S.F. (2010) The ODD protocol: A review and first update. *Ecological Modelling,* **221,** 2760-2768. 10.1016/j.ecolmodel.2010.08.019

592 Grimm, V., Railsback, S.F., Vincenot, C.E., Berger, U., Gallagher, C., DeAngelis, D.L., Edmonds,
593 B., Ge, J., Giske, J., Groeneveld, J., Johnston, A.S.A., Milles, A., Nabe-Nielsen, J., Polhill,
594 J.G., Radchuk, V., Rohwäder, M.-S., Stillman, R.A., Thiele, J.C. & Ayllón, D. (2020) The
595 ODD Protocol for Describing Agent-Based and Other Simulation Models: A Second Update
596 to Improve Clarity, Replication, and Structural Realism. *Journal of Artificial Societies and*
597 *Social Simulation,* **23**. 10.18564/jasss.4259

598 Grimm, V., Revilla, E., Berger, U., Jeltsch, F., Mooij, W.M., Railsback, S.F., Thulke, H.H., Weiner,
599 J., Wiegand, T. & DeAngelis, D.L. (2005) Pattern-oriented modeling of agent-based complex
600 systems: lessons from ecology. *Science,* **310,** 987-991. 10.1126/science.1116681

601 Gross, J.E. & Miller, M.W. (2001) Chronic Wasting Disease in Mule Deer: Disease Dynamics and
602 Control. *The Journal of Wildlife Management,* **65**. 10.2307/3802899

603 Habib, T.J., Merrill, E.H., Pybus, M.J. & Coltman, D.W. (2011) Modelling landscape effects on
604 density–contact rate relationships of deer in eastern Alberta: Implications for chronic wasting
605 disease. *Ecological Modelling,* **222,** 2722-2732. 10.1016/j.ecolmodel.2011.05.007

606 Haley, N.J. & Hoover, E.A. (2015) Chronic wasting disease of cervids: current knowledge and future
607 perspectives. *Annu Rev Anim Biosci,* **3,** 305-325. 10.1146/annurev-animal-022114-111001

608 Haley, N.J., Mathiason, C.K., Carver, S., Telling, G.C., Zabel, M.D. & Hoover, E.A. (2012)
609 Sensitivity of protein misfolding cyclic amplification versus immunohistochemistry in ante-
610 mortem detection of chronic wasting disease. *J Gen Virol,* **93,** 1141-1150.
611 10.1099/vir.0.039073-0

612 Hamlin, K.L. & Mackie, R.J. (1989) Mule deer in the Missouri River Breaks, Montana: a study of
613 population dynamics in a fluctuating environment.

614 Heisey, D.M., Osnas, E.E., Cross, P.C., Joly, D.O., Langenberg, J.A. & Miller, M.W. (2010) Linking
615 process to pattern: estimating spatiotemporal dynamics of a wildlife epidemic from cross-
616 sectional data. *Ecological Monographs,* **80,** 221-240. 10.1890/09-0052.1

617 Jackson, N.J., Stewart, K.M., Wisdom, M.J., Clark, D.A. & Rowland, M.M. (2021) Demographic
618 performance of a large herbivore: effects of winter nutrition and weather. *Ecosphere,* **12**.
619 10.1002/ecs2.3328

620 Jennelle, C.S., Henaux, V., Wasserberg, G., Thiagarajan, B., Rolley, R.E. & Samuel, M.D. (2014)
621 Transmission of chronic wasting disease in Wisconsin white-tailed deer: implications for
622 disease spread and management. *PLoS One,* **9,** e91043. 10.1371/journal.pone.0091043

623 Jennelle, C.S., Samuel, M.D., Nolden, C.A. & Berkley, E.A. (2009) Deer Carcass Decomposition
624 and Potential Scavenger Exposure to Chronic Wasting Disease. *Journal of Wildlife*
625 *Management,* **73,** 655-662. 10.2193/2008-282

626 Johnson, C.J., Herbst, A., Duque-Velasquez, C., Vanderloo, J.P., Bochsler, P., Chappell, R. &
627 McKenzie, D. (2011) Prion protein polymorphisms affect chronic wasting disease
628 progression. *PLoS One,* **6,** e17450. 10.1371/journal.pone.0017450

629 Johnson, R.T. (2005) Prion diseases. *The Lancet Neurology,* **4,** 635-642. 10.1016/S1474-
630 4422(05)70192-7

631 Kim, T.-Y., Shon, H.-J., Joo, Y.-S., Mun, U.-K., Kang, K.-S. & Lee, Y.-S. (2005) Additional Cases
632 of Chronic Wasting Disease in Imported Deer in Korea. *Journal of Veterinary Medical*
633 *Science,* **67,** 753-759. 10.1292/jvms.67.753

Kjaer, L.J. (2010) Individual-based modeling of white-tailed deer (*Odocoileus virginianus*) movements and epizootiology. Southern Illinois University Carbondale Carbondale, IL.

Lane-deGraaf, K.E., Kennedy, R.C., Arifin, S.M., Madey, G.R., Fuentes, A. & Hollocher, H. (2013) A test of agent-based models as a tool for predicting patterns of pathogen transmission in complex landscapes. *BMC Ecol,* **13,** 35. 10.1186/1472-6785-13-35

Lee, Y.-C.J. (2023) Prions: a threat to health security and the need for effective medical countermeasures. *Global Health Journal,* **7,** 43-48. 10.1016/j.glohj.2023.02.004

Lendrum, P.E., Anderson, C.R., Jr., Monteith, K.L., Jenks, J.A. & Bowyer, R.T. (2013) Migrating mule deer: effects of anthropogenically altered landscapes. *PLoS One,* **8,** e64548. 10.1371/journal.pone.0064548

Littell, J.S., Peterson, D.L., Riley, K.L., Liu, Y. & Luce, C.H. (2016) A review of the relationships between drought and forest fire in the United States. *Global Change Biology,* **22,** 2353-2369. https://doi.org/10.1111/gcb.13275

Loft, E.R. & Bleich, V.C. (2014) History of the conservation of critical deer ranges in California: concepts and terminology. *California Fish and Game,* **100,** 451-472.

Mackie, R.J. (1998) *Ecology and management of mule deer and white-tailed deer in Montana*. Montana Fish, Wildlife, and Parks, Wildlife Division.

Madadgar, S., Sadegh, M., Chiang, F., Ragno, E. & AghaKouchak, A. (2020) Quantifying increased fire risk in California in response to different levels of warming and drying. *Stochastic Environmental Research and Risk Assessment,* **34,** 2023-2031.

Mathiason, C.K., Hays, S.A., Powers, J., Hayes-Klug, J., Langenberg, J., Dahmes, S.J., Osborn, D.A., Miller, K.V., Warren, R.J., Mason, G.L. & Hoover, E.A. (2009) Infectious prions in pre-clinical deer and transmission of chronic wasting disease solely by environmental exposure. *PLoS One,* **4,** e5916. 10.1371/journal.pone.0005916

McCallum, H. (2016) Models for managing wildlife disease. *Parasitology,* **143,** 805-820. 10.1017/S0031182015000980

Mejia-Salazar, M.F., Goldizen, A.W., Menz, C.S., Dwyer, R.G., Blomberg, S.P., Waldner, C.L., Cullingham, C.I. & Bollinger, T.K. (2017) Mule deer spatial association patterns and potential implications for transmission of an epizootic disease. *PLoS One,* **12,** e0175385. 10.1371/journal.pone.0175385

Mejia Salazar, M.F. (2017) Social dynamics among mule deer and how they visit various environmental areas: implications for chronic wasting disease transmission. University of Saskatchewan.

Mejia Salazar, M.F., Waldner, C., Stookey, J. & Bollinger, T.K. (2016) Infectious Disease and Grouping Patterns in Mule Deer. *PLoS One,* **11,** e0150830. 10.1371/journal.pone.0150830

Miller, D.L., Alonzo, M., Meerdink, S.K., Allen, M.A., Tague, C.L., Roberts, D.A. & McFadden, J.P. (2022) Seasonal and interannual drought responses of vegetation in a California urbanized area measured using complementary remote sensing indices. *ISPRS Journal of Photogrammetry and Remote Sensing,* **183,** 178-195. https://doi.org/10.1016/j.isprsjprs.2021.11.002

Miller, M.W. & Conner, M.M. (2005) Epidemiology of Chronic Wasting Disease in free-ranging mule deer: spatial, temporal and demographic influences on observed prevalence patterns. *Journal of Wildlife Diseases,* **41,** 275-290. 10.7589/0090-3558-41.2.275

677 Miller, M.W., Hobbs, N.T. & Tavener, S.J. (2006) Dynamics of Prion Disease Transmission in Mule
678 Deer. *Ecological Applications,* **16,** 2208-2214. 10.1890/1051-
679 0761(2006)016[2208:Dopdti]2.0.Co;2

680 Miller, M.W., Swanson, H.M., Wolfe, L.L., Quartarone, F.G., Huwer, S.L., Southwick, C.H. &
681 Lukacs, P.M. (2008) Lions and prions and deer demise. *PLoS One,* **3,** e4019.
682 10.1371/journal.pone.0004019

683 Miller, M.W. & Williams, E.S. (2003) Prion disease: horizontal prion transmission in mule deer.
684 *Nature,* **425,** 35-36. 10.1038/425035a

685 Miller, M.W., Williams, E.S., Hobbs, N.T. & Wolfe, L.L. (2004) Environmental sources of prion
686 transmission in mule deer. *Emerg Infect Dis,* **10,** 1003-1006. 10.3201/eid1006.040010

687 Monteith, K.L., Bleich, V.C., Stephenson, T.R., Pierce, B.M., Conner, M.M., Kie, J.G. & Bowyer,
688 R.T. (2014) Life-history characteristics of mule deer: Effects of nutrition in a variable
689 environment. *Wildlife Monographs,* **186,** 1-62. 10.1002/wmon.1011

690 Monteith, K.L., Bleich, V.C., Stephenson, T.R., Pierce, B.M., Conner, M.M., Klaver, R.W. &
691 Bowyer, R.T. (2011) Timing of seasonal migration in mule deer: effects of climate, plant
692 phenology, and life-history characteristics. *Ecosphere,* **2**. 10.1890/es10-00096.1

693 Monteith, K.L., Hayes, M.M., Kauffman, M.J., Copeland, H.E. & Sawyer, H. (2018) Functional
694 attributes of ungulate migration: landscape features facilitate movement and access to forage.
695 *Ecol Appl,* **28,** 2153-2164. 10.1002/eap.1803

696 Mount, J., Escriva-Bou, A. & Sencan, G. (2021) Droughts in California. *Public Policy Institute of*
697 *California website, April. Accessed August,* **10,** 2022.

698 Munk, B. & Benedet, J. (2024) Chronic Wasting Disease Confirmed in California Deer Population—
699 CDFW Urges Hunters to be Vigilant and Participate in Disease Surveillance Efforts. *CDFW*
700 *News*. California Department of Fish and Wildlife, Sacramento, CA.

701 Muñoz, A.-R., Jiménez-Valverde, A., Márquez, A.L., Moleón, M. & Real, R. (2015) Environmental
702 favourability as a cost-efficient tool to estimate carrying capacity. *Diversity and*
703 *Distributions,* **21,** 1388-1400. https://doi.org/10.1111/ddi.12352

704 Mysterud, A. & Edmunds, D.R. (2019) A review of chronic wasting disease in North America with
705 implications for Europe. *European Journal of Wildlife Research,* **65**. 10.1007/s10344-019-
706 1260-z

707 National Wildlife Health Center (2024) Expanding Distribution of Chronic Wasting Disease
708 [accessed May 2024]. Available at https://www.usgs.gov/centers/nwhc/science/expanding-
709 distribution-chronic-wasting-disease

710 Osnas, E.E., Heisey, D.M., Rolley, R.E. & Samuel, M.D. (2009) Spatial and temporal patterns of
711 chronic wasting disease: fine-scale mapping of a wildlife epidemic in Wisconsin. *Ecol Appl,*
712 **19,** 1311-1322. 10.1890/08-0578.1

713 Otero, A., Velasquez, C.D., Aiken, J. & McKenzie, D. (2021) Chronic wasting disease: a cervid
714 prion infection looming to spillover. *Vet Res,* **52,** 115. 10.1186/s13567-021-00986-y

715 Plummer, I.H., Johnson, C.J., Chesney, A.R., Pedersen, J.A. & Samuel, M.D. (2018) Mineral licks as
716 environmental reservoirs of chronic wasting disease prions. *PLoS One,* **13,** e0196745.
717 10.1371/journal.pone.0196745

Plummer, I.H., Wright, S.D., Johnson, C.J., Pedersen, J.A. & Samuel, M.D. (2017) Temporal patterns of chronic wasting disease prion excretion in three cervid species. *J Gen Virol,* **98,** 1932-1942. 10.1099/jgv.0.000845

Potapov, A., Merrill, E., Pybus, M., Coltman, D.W. & Lewis, M.A. (2013) Chronic wasting disease: Possible transmission mechanisms in deer. *Ecological Modelling,* **250,** 244-257. 10.1016/j.ecolmodel.2012.11.012

Potapov, A., Merrill, E., Pybus, M. & Lewis, M.A. (2016) Chronic Wasting Disease: Transmission Mechanisms and the Possibility of Harvest Management. *PLoS One,* **11,** e0151039. 10.1371/journal.pone.0151039

Rittenhouse, C.D., Mong, T.W. & Hart, T. (2015) Weather conditions associated with autumn migration by mule deer in Wyoming. *PeerJ,* **3,** e1045. 10.7717/peerj.1045

Robinette, W.L. (1966) Mule Deer Home Range and Dispersal in Utah. *The Journal of Wildlife Management,* **30**. 10.2307/3797822

Schuyler, E.M., Dugger, K.M. & Jackson, D.H. (2018) Effects of distribution, behavior, and climate on mule deer survival. *The Journal of Wildlife Management,* **83,** 89-99. 10.1002/jwmg.21558

Shellard, A. & Mayor, R. (2020) Rules of collective migration: from the wildebeest to the neural crest. *Philosophical Transactions of the Royal Society B: Biological Sciences,* **375,** 20190387. doi:10.1098/rstb.2019.0387

Sparks, A.M., Kolden, C.A., Smith, A.M.S., Boschetti, L., Johnson, D.M. & Cochrane, M.A. (2018) Fire intensity impacts on post-fire temperate coniferous forest net primary productivity. *Biogeosciences,* **15,** 1173-1183. 10.5194/bg-15-1173-2018

Spraker, T., Miller, M., Williams, E., Getzy, D., Adrian, W., Schoonveld, G., Spowart, R., O'Rourke, K.I., Miller, J. & Merz, P. (1997) Spongiform encephalopathy in free-ranging mule deer (*Odocoileus hemionus*), white-tailed deer (*Odocoileus virginianus*) and Rocky Mountain elk (*Cervus elaphus nelsoni*) in northcentral Colorado. *Journal of Wildlife Diseases,* **33,** 1-6. 10.7589/0090-3558-33.1.1

Stanke, H., Jaffe, N., Xie, Y. & Ligmann-Zielinska, A. (2018) An agent based modelling approach to estimate dispersal potential of white tailed deer: Implications for Chronic Wasting Disease. *GEO 869 Geosimulation* pp. 11. Michigan State University, Michigan.

Storm, D.J., Samuel, M.D., Rolley, R.E., Shelton, P., Keuler, N.S., Richards, B.J. & Van Deelen, T.R. (2013) Deer density and disease prevalence influence transmission of chronic wasting disease in white-tailed deer. *Ecosphere,* **4,** 1-14. 10.1890/es12-00141.1

Taillandier, P., Gaudou, B., Grignard, A., Huynh, Q.-N., Marilleau, N., Caillou, P., Philippon, D. & Drogoul, A. (2018) Building, composing and experimenting complex spatial models with the GAMA platform. *GeoInformatica,* **23,** 299-322. 10.1007/s10707-018-00339-6

Tamguney, G., Miller, M.W., Wolfe, L.L., Sirochman, T.M., Glidden, D.V., Palmer, C., Lemus, A., DeArmond, S.J. & Prusiner, S.B. (2009) Asymptomatic deer excrete infectious prions in faeces. *Nature,* **461,** 529-532. 10.1038/nature08289

Taylor, T.J. (1996) Condition and reproductive performance of female mule deer in central Sierra Nevada. *California Fish and Game,* **82,** 122-132.

Towne, E.G. (2000) Prairie vegetation and soil nutrient responses to ungulate carcasses. *Oecologia,* **122,** 232-239. 10.1007/PL00008851

Valente, A.M., Acevedo, P., Figueiredo, A.M., Fonseca, C. & Torres, R.T. (2020) Overabundant wild ungulate populations in Europe: management with consideration of socio-ecological consequences. *Mammal Review,* **50,** 353-366. 10.1111/mam.12202

van de Kerk, M., Larsen, R.T., Olson, D.D., Hersey, K.R. & McMillan, B.R. (2021) Variation in movement patterns of mule deer: have we oversimplified migration? *Mov Ecol,* **9,** 44. 10.1186/s40462-021-00281-7

van Mantgem, E.F., Keeley, J.E. & Witter, M. (2015) Faunal Responses to Fire in Chaparral and Sage Scrub in California, USA. *Fire Ecology,* **11,** 128-148. 10.4996/fireecology.1103128

Walker, M.A., Uribasterra, M., Asher, V., Ponciano, J.M., Getz, W.M., Ryan, S.J. & Blackburn, J.K. (2020) Ungulate use of locally infectious zones in a re-emerging anthrax risk area. *R Soc Open Sci,* **7,** 200246. 10.1098/rsos.200246

Wasserberg, G., Osnas, E.E., Rolley, R.E. & Samuel, M.D. (2009) Host culling as an adaptive management tool for chronic wasting disease in white-tailed deer: a modelling study. *J Appl Ecol,* **46,** 457-466. 10.1111/j.1365-2664.2008.01576.x

Webb, G.K. (2013) Deer herd management using the internet: a comparative study of California targeted by data mining the internet. *Issues in Information Systems***,** 156.

White, G.C., Freddy, D.J., Gill, R.B. & Ellenberger, J.H. (2001) Effect of Adult Sex Ratio on Mule Deer and Elk Productivity in Colorado. *The Journal of Wildlife Management,* **65**. 10.2307/3803107

Williams, E.S. (2005) Chronic wasting disease. *Vet Pathol,* **42,** 530-549. 10.1354/vp.42-5-530

Williams, E.S. & Young, S. (1980) Chronic wasting disease of captive mule deer: a spongiform encephalopathy. *Journal of Wildlife Diseases,* **16,** 89-98. 10.7589/0090-3558-16.1.89

Winter, S.N. & Escobar, L.E. (2020) Chronic Wasting Disease Modeling: An Overview. *J Wildl Dis,* **56,** 741-758. 10.7589/2019-08-213

Wood, A.K., Hamlin, K.L., Mackie, R.J. & Montana. Wildlife, D. (1989) *Ecology of sympatric populations of mule deer and white-tailed deer in a prairie environment*. Wildlife Division, Montana Dept. of Fish, Wildlife & Parks, [S.l.].

Xu, J., Merrill, E.H. & Lewis, M.A. (2022) Spreading speed of chronic wasting disease across deer groups with overlapping home ranges. *J Theor Biol,* **547,** 111135. 10.1016/j.jtbi.2022.111135

Zipf, G.K. (1949) *Human behavior and the principle of least effort*. Addison-Wesley Press, Oxford, England.

792